Journal of
Micro/Nanolithography,
MEMS, and MOEMS

Nanolithography.SPIEDigitalLibrary.org

Influence of secondary effects in the fabrication of submicron resist structures using deep x-ray lithography

Abrar Faisal
Thomas Beckenbach
Jürgen Mohr
Pascal Meyer

SPIE.

Abrar Faisal, Thomas Beckenbach, Jürgen Mohr, Pascal Meyer, "Influence of secondary effects in the fabrication of submicron resist structures using deep x-ray lithography," *J. Micro/Nanolith. MEMS MOEMS* **18**(2), 023502 (2019), doi: 10.1117/1.JMM.18.2.023502.

Influence of secondary effects in the fabrication of submicron resist structures using deep x-ray lithography

Abrar Faisal,[a] Thomas Beckenbach,[b] Jürgen Mohr,[a] and Pascal Meyer[a,*]
[a]Karlsruhe Institute of Technology, Institute of Microstructure Technology, Eggenstein-Leopoldshafen, Germany
[b]microworks GmbH, Karlsruhe, Germany

Abstract

Background: Deep x-ray lithography using synchrotron radiation is a prominent technique in the fabrication of high aspect ratio microstructures. The minimum lateral dimensions producible are limited by the primary dose distribution and secondary effects (Fresnel diffraction, secondary electrons scattering, etc.) during exposure.

Aim: The influence of secondary radiation effects on the fabrication of high aspect ratio microstructures with submicrometer lateral dimension by deep x-ray lithography is characterized.

Approach: The microstructures under investigation are one-dimensional gratings. The influence of secondary effects on structural dimension is simulated and compared to the experimental results. The quality criteria and possible defects arising in experiments highlight the importance of the mechanical stability of the photoresist.

Results: From the simulation results, the minimum period of microstructures that can be produced is about 600 nm. Experimentally, microstructures with 1.2 μm minimum period (resist width of ~700 nm) and height of ~10 μm could be fabricated.

Conclusions: Simulation results show the feasibility for fabricating gratings with a period less than 1 μm. To achieve these values also in experiment, it is necessary to increase the mechanical stability of the high aspect lamellae. The outcome of these results allows one to reduce the expensive and lengthy product development cycle.

 [DOI: 10.1117/1.JMM.18.2.023502]

Keywords: x-ray lithography; sub-μm structure; dose deposition simulation; one-dimensional grating; phase contrast.

Paper 19008 received Feb. 1, 2019; accepted for publication Apr. 16, 2019; published online May 15, 2019.

1 Introduction

For more than 20 years, research has focused on using deep x-ray lithography[1–3] for fabricating microstructures with high precision features, dimensions, and quality, which would otherwise not be feasible using conventional methods. Submicrometer hole structures with diameters 750 to 890 nm and ~10 μm thick were patterned in an epoxy-based negative resist using soft x-ray lithography.[4] Polymer test structures with lateral dimensions in the submicron regime have also been attempted on PMMA[5] (500-nm wide and 5-μm thick).

In x-ray phase contrast imaging techniques[6–8] with lab sources using a Talbot-Lau interferometer, one-dimensional (1-D) gratings are the primary optical components. Reznikova et al.[9] demonstrated the process to fabricate 2-μm period grating (60 μm thick) on SU-8 layers using x-ray lithography, with the use of a beam-stop, which makes the irradiation process complex and furthermore nonreproducible.

Grating periods in the sub-μm scale are necessary to aim toward higher resolution imaging, higher sensitivity as well as compact setup sizes (<1 m). In this paper, we present a study of simulated and experimental results to explore the possibilities for patterning 1-D grating microstructures with period down to 1.0 μm, using standard and repeatable exposure conditions. The thickness of the photoresist layer is set to 10 μm and a negative epoxy resin (mr-X, micro resist technology GmbH) is used. The experiments were performed at the LIGA-1 beamline of the ANKA/KARA synchrotron facility (KIT, Germany). First, the simulation results will be presented. Deviations in the geometry of intended structure pattern are created due to an undesirable dose distribution in both the shadowed and exposed regions of the resist.[10] In the second part, the experimental results will be described. The final part concerns the comparison between the results from the experiment and simulation. The outcome of these results allows reduction of expensive and lengthy product development cycle times.

2 Effects in X-Ray Irradiation

In the first step of the LIGA process,[3] an x-ray-sensitive polymer layer of up to several millimeters thickness is coated onto a substrate. Typically, PMMA is used as positive resist and an epoxy-based resin such as SU-8[11] as negative resist. The pattern of an x-ray mask is transferred onto the photoresist layer using x-rays from synchrotron radiation. After exposure, a replica of the mask pattern is obtained after dissolution of the chemically modified irradiated parts of the positive resist (or nonirradiated parts of the negative resist) in a chemical developer solution. Depending on the application, the polymer template is used in a following electroforming process to build metal structures, e.g., out of gold or nickel. When the x-ray photons penetrate and further interact

*Address all correspondence to Pascal Meyer, E-mail: pascal.meyer@kit.edu

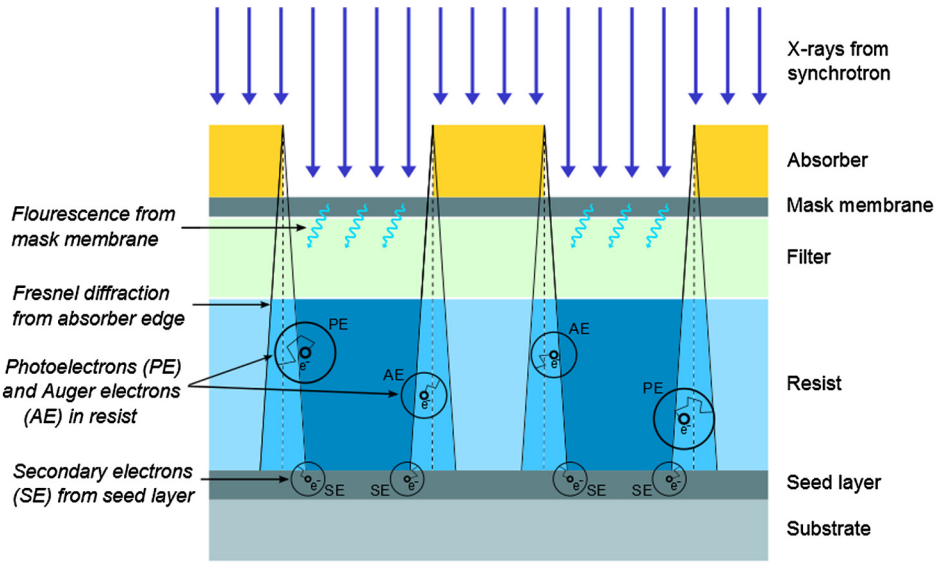

Fig. 1 Schematic illustration of the secondary effects during deep x-ray exposure (included in DoseSim) (adapted from Fig. 5 of Ref. 13).

with the resist material, they produce photoelectrons and Auger electrons within the material, which react with the resist to initiate the chemical modifications. These electrons gradually lose their energy through collisions with the resist molecules; their range increases with increasing initial energy. Thus, these (i) Auger/photoelectrons introduce secondary effects when they reach the unexposed regions leading to reduced edge sharpness. Other secondary effects that should be considered in calculating the deposited dose in the resist include (ii) Fresnel diffraction at an absorber edge, (iii) secondary electrons from the layer between the resist and substrate, and (iv) fluorescence radiation from the mask membrane and the seed layer. These effects are shown in Fig. 1 (for a periodic grating structure), and they are already implemented in the DoseSim program.[12]

We show by simulation that the effect of Fresnel diffraction, in case of a low proximity distance, on the change in structural widths is small enough to be neglected and it simplifies the deposited dose calculations. Any fluorescence radiation from the mask membrane, substrate material, or the adhesive seed layer are not existing as the photon energies in the x-ray beam are less than the K-edge of these materials, after being filtered by the mirror optics implemented in the beamline under consideration. Any photoelectrons generated from the titanium mask membrane are blocked using thin Kapton filters. Therefore, for the calculations presented here, we took into account only the photoelectrons generated in the resist, and in the seed layer at the resist/substrate interface.

3 Simulation and Experimental Parameters

3.1 *Photoresist and Substrate*

The photoresist used in the experiments is a SU-8-based epoxy resin formulation called mr-X (micro resist technology GmbH) with additives to improve stability, sensitivity, and adhesion properties. Two versions, namely mr-X 10 and mr-X 50, are used actually in deep x-ray lithography to fabricate microstructures. The mr-X 10 resist has more solvent content compared to the mr-X 50 and is *de facto* more applicable for structuring thin resist layers, which is the case here. A standard characterization of these formulations is performed by the method described in Ref. 14, which is used to determine the contrast. The contrast will be translated here as dose threshold; higher contrast corresponding to a higher threshold. The wafers used are 4-in. silicon substrates with a thickness of 200 or 525 μm and coated with an oxidized 2.5-μm titanium layer. The samples are spin-coated with 10 μm resist and stored for 4 to 5 days before exposure to allow the coated resist layer to settle.

3.2 *Exposure and Postprocess*

The x-ray irradiations are performed at the LIGA-1 beamline of the ANKA/KARA synchrotron facility (KIT, Germany). The synchrotron has electron beam energy of 2.5 GeV and the beamlines are situated on a bending magnet (1.5T). The LIGA-1 beamline is equipped with a chromium single mirror; a grazing incidence angle of 15.4 mrad is used, cutting off x-ray photons with energies larger than 5 keV[3]. A 7.5-μm thin film of polyimide is used between the mask and resist (sample) to absorb the photoelectrons from the titanium mask membrane. The standard bottom-dose used is 140 J/cm^3 as it has been identified in x-ray gratings fabrication (LIGA-1) with the mr-X resist. The required exposure dose (in mA.min/cm) for the specific parameters is calculated using the DoseSim[12] program. The exposure parameters are summarized in Table 1. A postexposure bake (PEB) is done at 65°C for the final curing of the samples. For the samples development, the freeze drying technique is used.[15]

4 Simulation

The simulations are performed using the DoseSim program, which includes the special features critical to deep x-ray lithography. The system calculates the spatial distribution of the x-ray dose deposited into the resist with and without the absorber and at the interface between resist and substrate (seed layer).

Table 1 Exposure parameters for analysis of sub-μm periodic structures.

Synchrotron source	ANKA/KARA (KIT)
Beamline	LIGA-1
Energy spectrum	2 to 4 keV
Mask membrane	Titanium (Ti) 2.5 μm
Absorber thickness	Gold (Au) 1 μm
Filter mask/resist interface	Polyimide film 7.5 μm
Resist	mr-X 10
Proximity (distance mask-resist)	Less than 20 μm
Bottom-dose	140 J/cm^3 (or 100 J/cm^3)

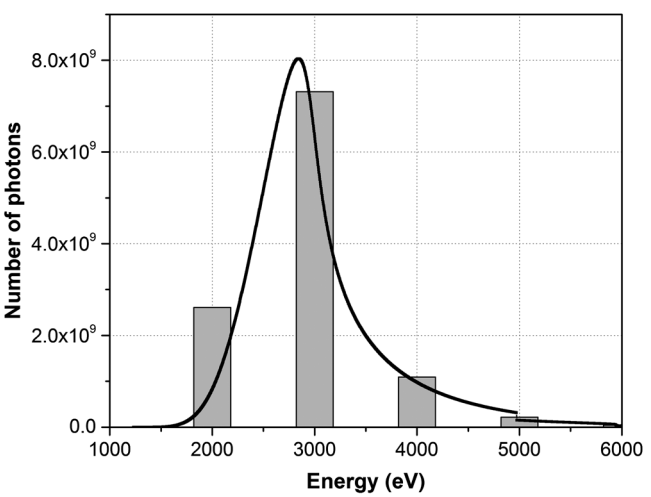

Fig. 2 Discretization of ANKA LIGA-1 spectrum (100 nm $\times$ 100 nm unit cells).

4.1 *Spectrum Discretization and Fresnel Diffraction*

The low x-ray energy spectrum (2 to 4 keV) at the ANKA LIGA-1 beamline is most suitable for the fabrication of sub-μm periodic microstructures with periods smaller than 2 μm and with heights of several 10 μm owing to the high energy photons cut-off by the installed mirror optics. DoseSim uses a discrete spectrum, which is a function of the resist unit cell size (10 nm $\times$ 10 nm or 100 nm $\times$ 100 nm). For our purpose, only the 100-nm unit cell size could be employed. The discretization of the spectrum used in the simulation, after the mask and filter, is presented in Fig. 2. For the resist material, the data for the positive resist PMMA have been used; the data calculations for the negative resist are still in progress. Nevertheless, first calculations show that the point spread function of the dose deposition is comparable.

In Fig. 3, a comparison of the contribution of Fresnel diffraction in the case of the proximity in the order of 20 μm is shown. For simplicity, the simulation has been done for 3-keV monoenergetic source (majority of photons with this energy, see Fig. 2), 10-μm thick resist, 10-μm proximity between mask and resist layer and 1-μm Au absorber thickness. A sideview of part of the dose distribution (width) is shown for the 10-μm resist thickness (depth) when exposed from the top. The dose spreads out decreasingly from the exposed region (right) to the shadowed region (left). The white lines are the iso-dosis-lines labeled with the actual dose values in J/cm^3. Two iso-dosis-lines are represented (35 and 10 J/cm^3); these values represent the threshold between completely developed and undeveloped photoresist (mr-X-10). The difference in position is less than 3%, resulting in comparable widths achieved after exposure. Therefore, in the following simulation results, the effect of Fresnel diffraction has been ignored due to its negligible contribution in the final microstructure dimensions.

4.2 *Results*

As an example, the simulation results of the influence of the photoelectrons generated in the resist on the dose deposition for a 1.4-μm periodic structure are presented in Fig. 4. A simple periodic structure, where an absorbing region (metal) is present in between two nonabsorbing regions (resist) is

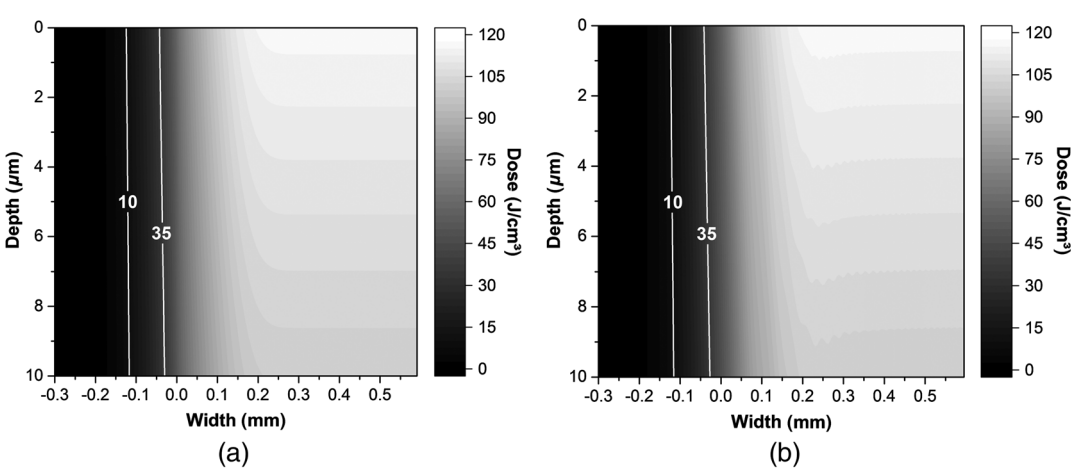

Fig. 3 Comparison of the effect of Fresnel diffraction on structural widths by simulation (3-keV monoenergetic source, 10-μm resist, 10-μm proximity, and 10-μm Au absorber) (a) with diffraction and (b) without diffraction.

simulated. The iso-dosis-line values are decreasing while spreading outward from the exposed region to the region underneath the absorber, with maximum dose at the center of the exposed areas. Due to the secondary effects, the increased dose underneath the absorber could initiate unwanted crosslinking of the resist in the shadowed region, which is intended to be developed completely for subsequent electroforming of metals. The iso-dosis-lines are labeled with the actual dose values in 0.01 J/cm^3.

By choosing a crosslinking threshold of 35 J/cm^3, the opening region width decreases by 100 nm (700 to 600 nm). Decreasing the threshold to 10 J/cm^3, the simulated width is 300 nm smaller. Therefore, it should be possible to fabricate gratings with such periods, without having residual resist in the unexposed region. However, the width of the unexposed region is decreasing as a function of the resist contrast, and thus a duty cycle (DC) of 0.4 and 0.3 compared to the design value of 0.5, will be obtained for the threshold 35 and 10 J/cm^3, respectively.

To obtain a DC of 0.5 for the copy of the mask, the DC of the mask should be increased. In Fig. 5, a simulation of a DC 0.64 (absorber width is 0.9 μm) is presented. In this case, a DC of 0.43 will be matched for the threshold 10 J/cm^3.

One important fact is that the decrease of the width is constant (100 and 300 nm), and it is independent of the width of the absorber. This will be true until the dose deposition can reach a plateau; using LIGA-1 this plateau is reached for a width of 0.4 μm. Below this value, the decrease will increase until the difference will be 0. By reducing the bottom-dose, the resist opening width will be increased for a given threshold. For example, by reducing the bottom-dose from 140 to 100 J/cm^3, the width is increased by 20 and 30 nm in the case of the 1.4-μm period with DC 0.5 (see Fig. 6).

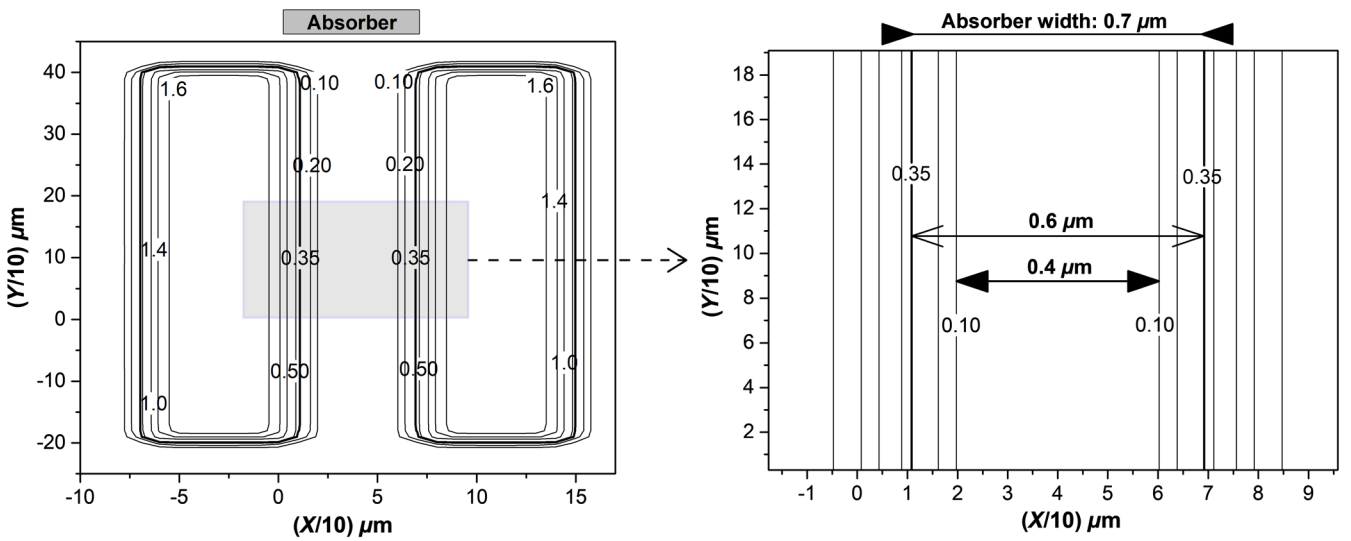

Fig. 4 Iso-dosis-lines of 1.4 μm periodic structure with DC of 0.5. The values on the iso-dosis-lines indicate the actual dose in 0.01 J/cm^3. The Au absorber thickness is 1 μm. The calculated bottom dose is 140 J/cm^3.

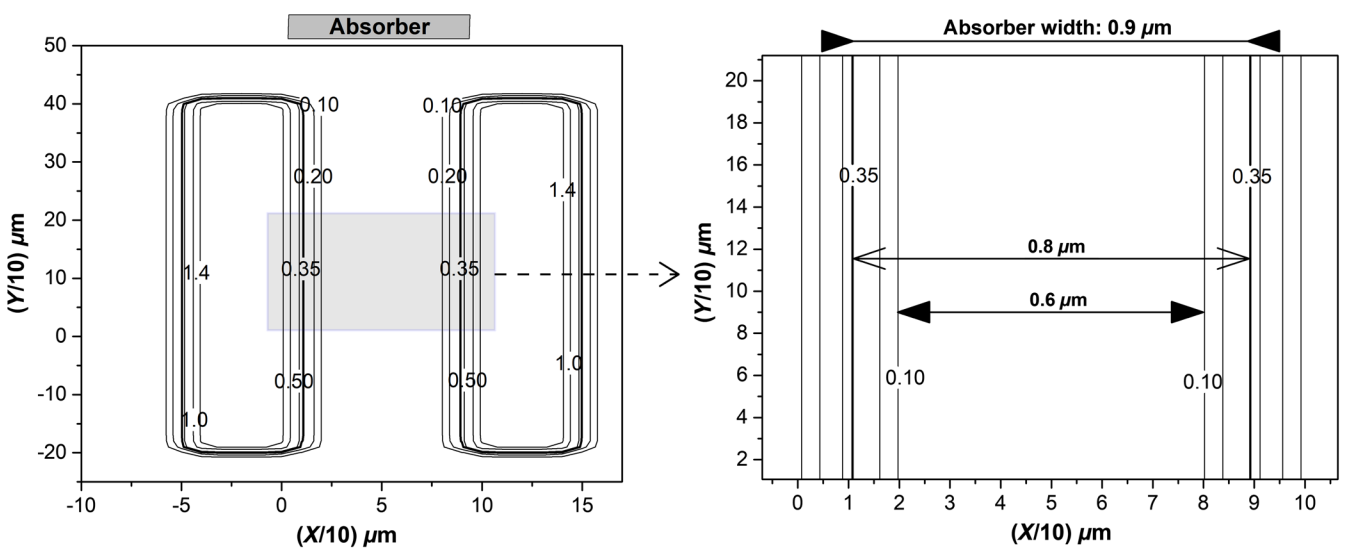

Fig. 5 Iso-dosis-lines of 1.4 μm periodic structure with DC of 0.64. The values on the iso-dosis-lines indicate the actual dose in 0.01 J/cm^3. The Au absorber thickness is 1 μm. The calculated bottom dose is 140 J/cm^3.

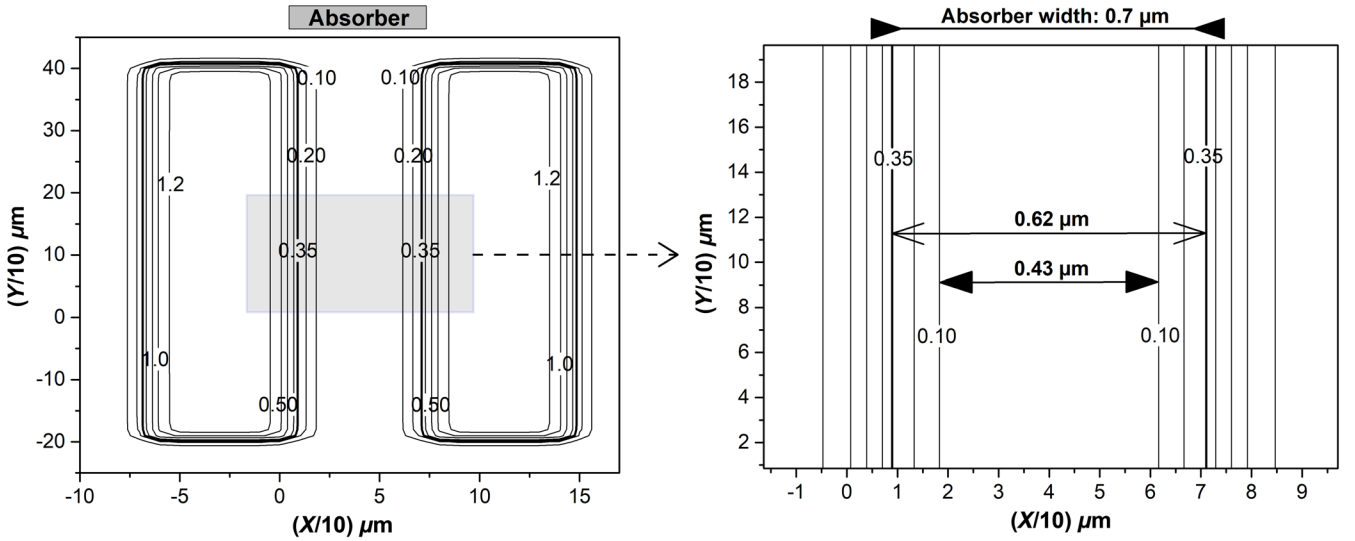

Fig. 6 Iso-dosis-lines of 1.4 μm periodic structure with DC of 0.5. The values on the iso-dosis-lines indicate the actual dose in 0.01 J/cm^3. The Au absorber thickness is 1 μm. The calculated bottom dose is 100 J/cm^3.

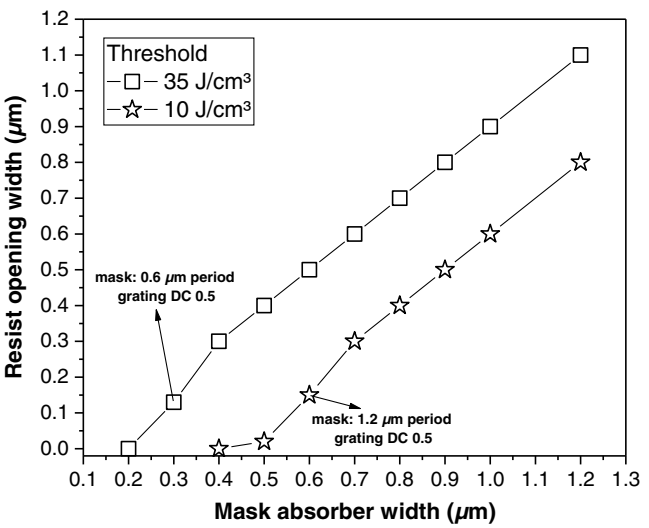

Fig. 7 Simulation of resist opening width against mask Au absorber width. The calculated bottom dose is 140 J/cm^3.

As a summary, in Fig. 7, the simulated results for the two different thresholds are plotted, with 140 J/cm^3 as bottom-dose. The Au absorber width versus resist opening width is linear; this quality is not anymore present when the absorber mask width is so small that the deposited dose in the two irradiated parts overlaps. From these results, the minimum period will be in the range of 0.6 to 1.2 μm (DC: 0.5 for the mask), by using the two different thresholds. By reducing the exposure dose, this minimum period could be slightly reduced.

5 Experiments

5.1 *Test Microstructures*

To compare/validate the simulated results and experimentally realize the possibilities to fabricate sub-μm structures, at first, a 2.5-μm titanium membrane mask was fabricated

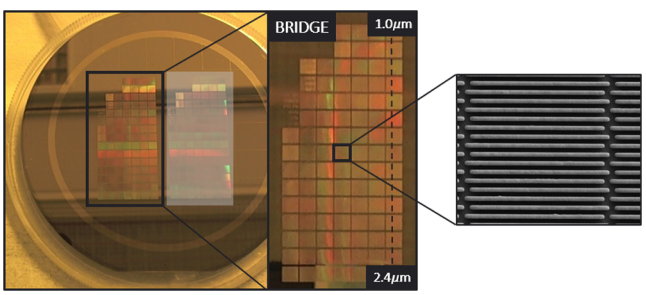

Fig. 8 Test fields arrangement for experimental realization of sub-μm microstructures using deep x-ray lithography (the missing structure fields in the top-left could not be fabricated by E-beam lithography due to their low DC and period).

using E-beam lithography. The thickness of gold absorber structures is in the range of 0.65 to 1 μm. The design includes 1-D grating fields (2.5 mm $\times$ 2.5 mm) with periods from 2.4 μm down to 1.0 μm in 0.1 μm steps. There were seven fields for each period; each field presenting a different ratio between metal/resist opening and period of structures (DC), between 0.4 and 0.8. The image in Fig. 8 shows the arrangement of the various fields, with an example scanning electron microscope (SEM) image showing the Au structures. The lines are 20 μm long, with gaps/breaks in between (equal to the width of the line). These gaps act as support bridges for stability of the resist lamellae.

5.2 *Results*

Several aspects throughout the x-ray lithography process can influence the final quality of the microstructures. These include the mechanical stability and adhesion of the photoresist on a particular surface, the exposure dose that is applied during x-ray lithography, the adhesion promoting seed layer used between the photoresist and the substrate, the process of electroforming related to the desired metal to deposit, etc.

The parameters investigated concern one type of layer (TiOx) and one thickness (10 μm); the experiment is completed after the development process (no electroforming).

The characterization is performed using a SEM and the lateral measurements executed using an in-house developed program for the period and DC. The samples are sputtered with 20-nm gold layer for better imaging.

5.2.1 *Quality criteria of 1-D grating microstructures*

The mechanical stability of the microstructures is an important innate characteristic of the formulation of the photoresist. It depends on the level of adhesion that is achieved on a specific layer or wafer surface, on the dose gradient, and the stresses induced during the PEB.

The resist lamellae should be straight as in Fig. 9(a). When all the parameters are not well chosen, the microstructures can undergo defects such as sticking, waviness, and crosslinking in the shadowed regions. Waviness could be due to inadequate resist crosslinking and/or poor adhesion [Fig. 9(b)]. Sticking may arise from the same conditions plus due to improper development and drying of the samples [Fig. 9(c)]. Crosslinking in the shadowed regions may be due to overexposure of the samples [Fig. 9(d)]. Any shifts in the

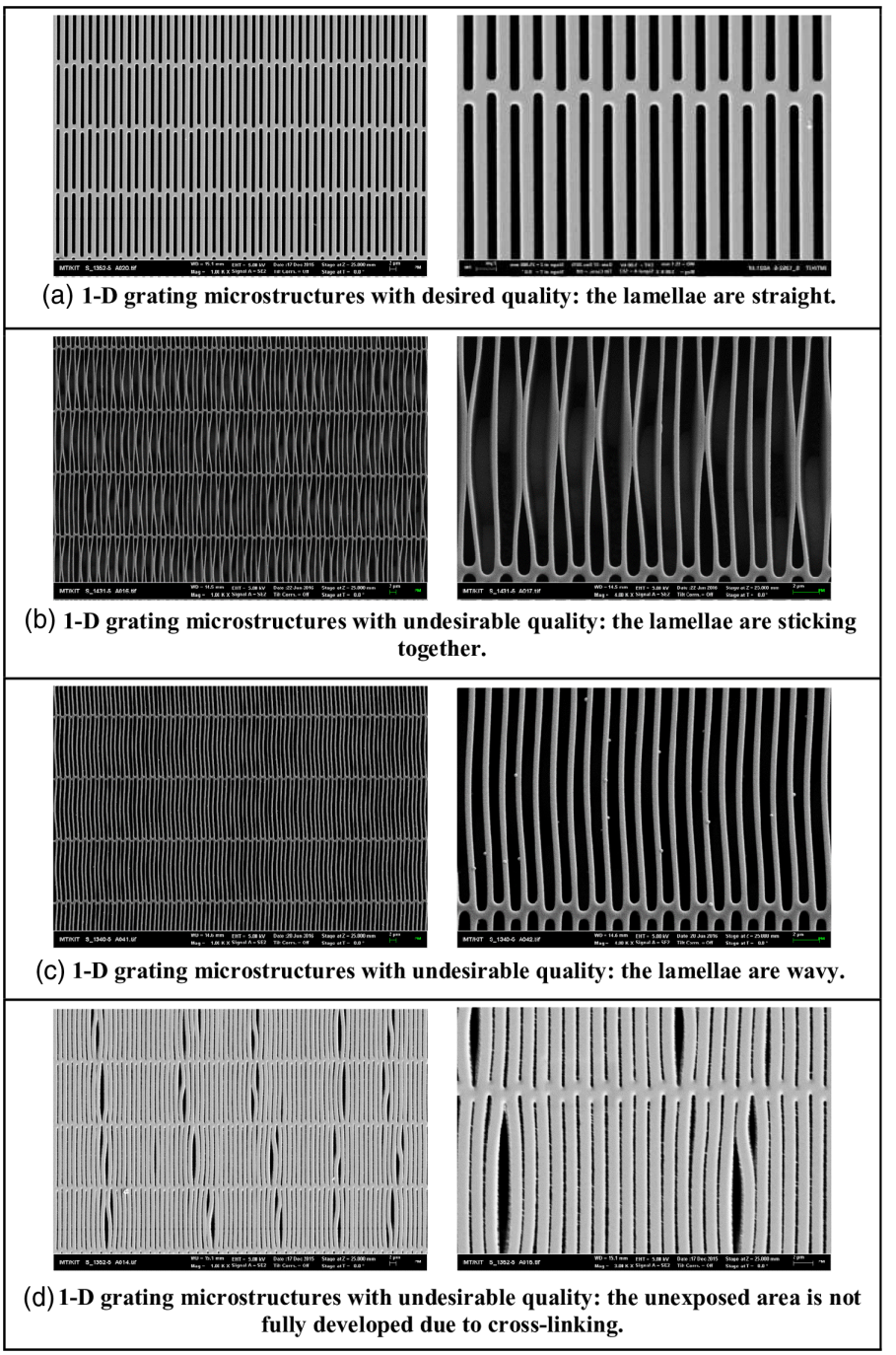

Fig. 9 Quality criteria of test microstructures using deep X-ray lithography including (a) ideal quality, (b) sticking, (c) waviness, and (d) crosslinking in the unexposed part and cracks in the resist lamellae.

Table 2 List of samples with the variable parameters of bottom-dose and resist batches.

Sample	Bottom-dose, BD (J/cm^3)	mr-X 10 batch
Sample-1	140	Batch-1
Sample-2	140	Batch-2
Sample-3	140	Batch-2
Sample-4	100	Batch-1
Sample-5	100	Batch-2

sensitivity/contrast of the photoresist also mean incorrect estimation of the required dose for resist crosslinking and therefore introduces defects in the final microstructures.

5.2.2 *Variation of bottom dose and contrast*

The influence of the exposure dose (different doses) applied during x-ray lithography on the gratings quality is analyzed by applying different doses, while the other process parameters are kept the same (resist coating, baking, development, etc.). In addition, samples prepared with the same photoresist formulation (mr-X 10) but different supplied batches (batch-1 and -2) were also compared. Table 2 lists the samples with the variable parameters used.

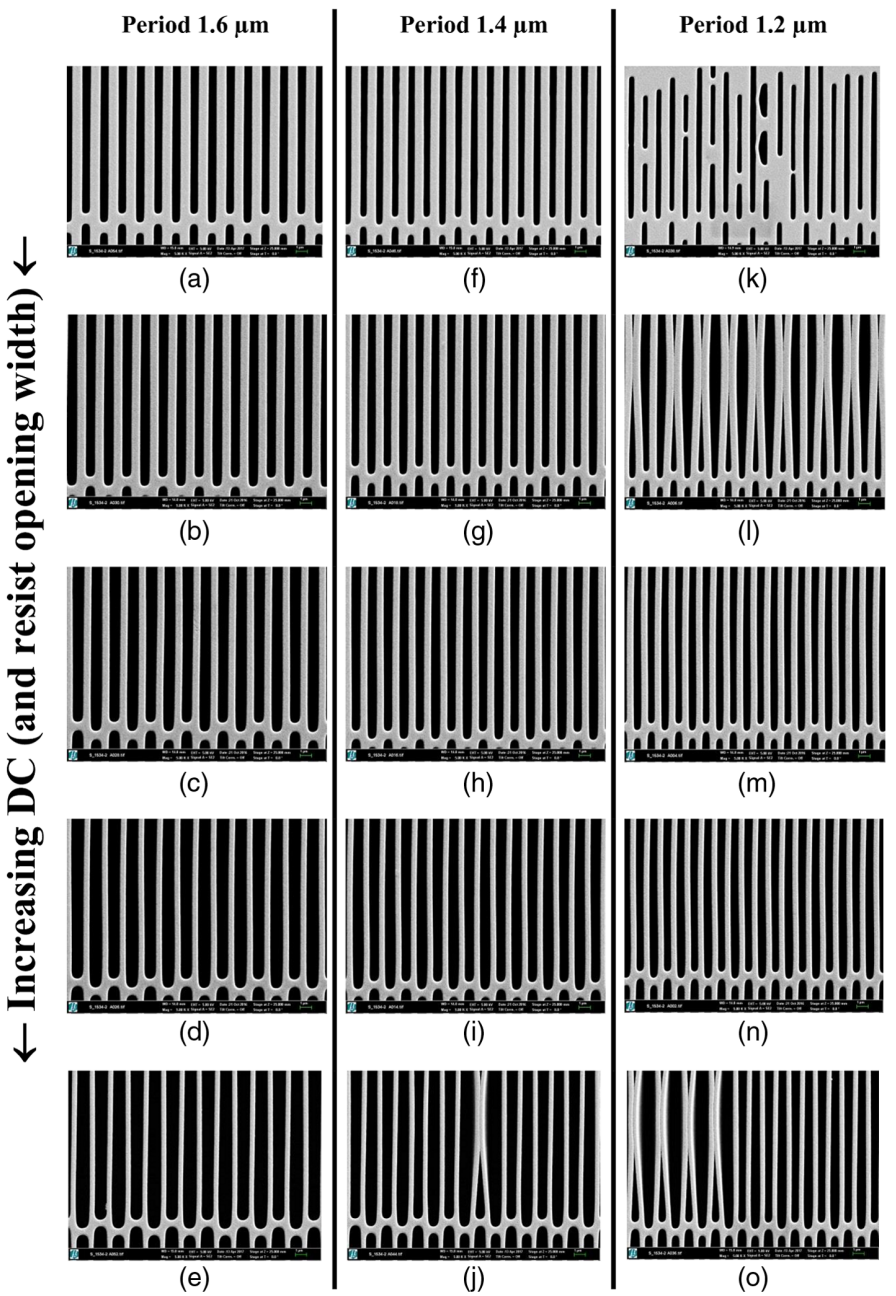

Fig. 10 Overview of SEM images of periodic microstructures with period (a)–(e) 1.6 μmwith increasing DC, (f)–(j) 1.4 μm with increasing DC, and (k)–(o) 1.2 μm with increasing DC; for resist thickness of ↑0 μm (sample-2). Defects from the mask transferred to resist in (k). Random sticking of resist lamellae in (j), (l), and (o)

Exemplarily, an overview of the fields from sample-2 for 1.6, 1.4, and 1.2 μm periods with different DC (five for each period) is shown in Fig. 10. The defects seen in field (*k*) are due to mask defects. Some random sticking of lamellae is seen in few fields as (j), (l), and (o). With a minimum period of 1.2 μm, resist structural width of ~450 nm (AR 22) is achieved, which is almost at the limit of being mechanically stable [Fig. 10(o)].

In Figs. 11 and 12, the relation between the mask absorber widths and the resulting resist opening widths on the sample is plotted for various periodic fields from sample-1 and sample-2 (same bottom-dose 140 J/cm^3). The relationship is relatively linear and independent of the period, as it was pointed out in the simulation for the same exposure parameters.

However, for the samples prepared from different resist batches, a change in the resist contrast can be observed. In Fig. 13, a comparison concerning the 1.4-μm period for sample-1, sample-2, and sample-3 shows clearly this difference between batch-1 (sample-1) and batch-2 (sample-2 and sample-3). Sample-1 presents a lower contrast, which results in a higher crosslinking in the unexposed part, producing thicker resist lamellae (smaller openings). The difference in structural widths due to difference in resist contrast of batch-1 and batch-2 is between 7% and 16%.

Two bottom-doses 100 and 140 J/cm^3 are tested in case of two sets of samples prepared with different batches. Figure 14 presents the 1.4-μm period measurement comparison of sample-1 (BD 140 J/cm^3) and sample-4 (BD 100 J/cm^3) using batch-1 and in Fig. 15 the comparison of sample-2 (BD 140 J/cm^3) and sample-5 (BD 100 J/cm^3) using batch-2.

In both cases (batch-1 and batch-2), as expected, a lower bottom-dose of 100 J/cm^3 (sample-4 and sample-5) produces wider resist openings. The difference observed is not linear: ~16% larger resist opening (110 nm) is achieved for

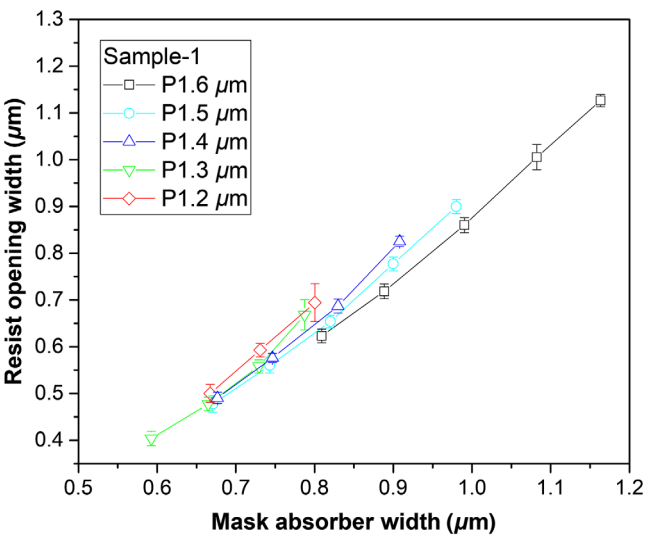

Fig. 11 Graphical representation of resist opening widths achieved from corresponding absorber widths on the mask from sample-1.

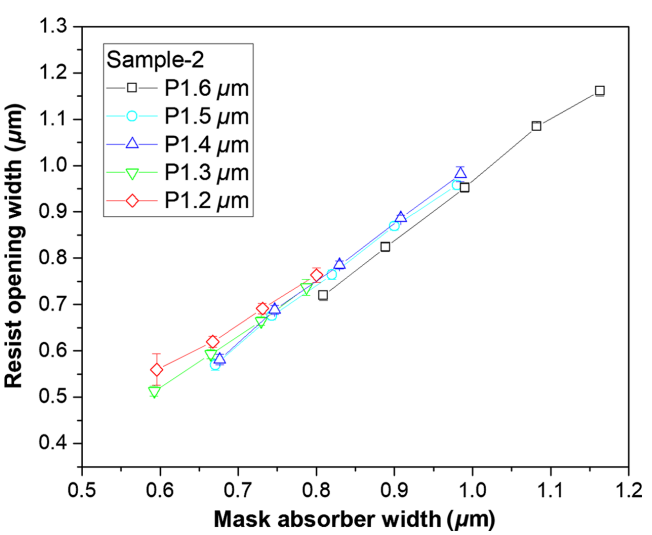

Fig. 12 Graphical representation of resist opening widths achieved from corresponding absorber widths on the mask from sample-2.

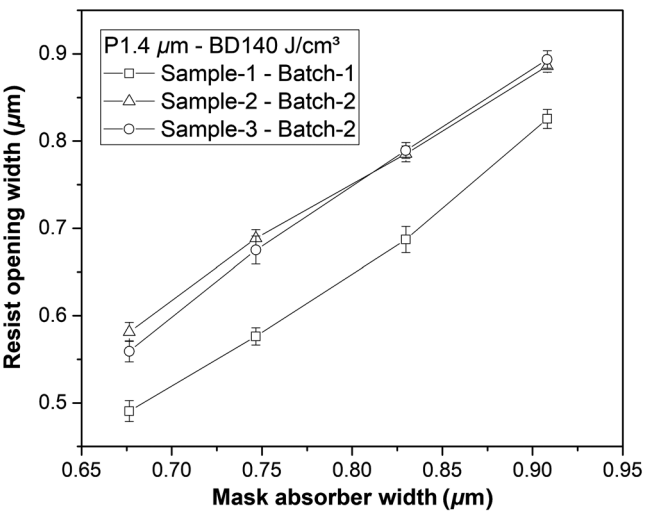

Fig. 13 Graphical comparison of resist opening widths achieved from corresponding absorber widths on the mask for period 1.4 μm fields between sample-1, sample-2, and sample-3 prepared from two resist batches (batch-1 and batch-2).

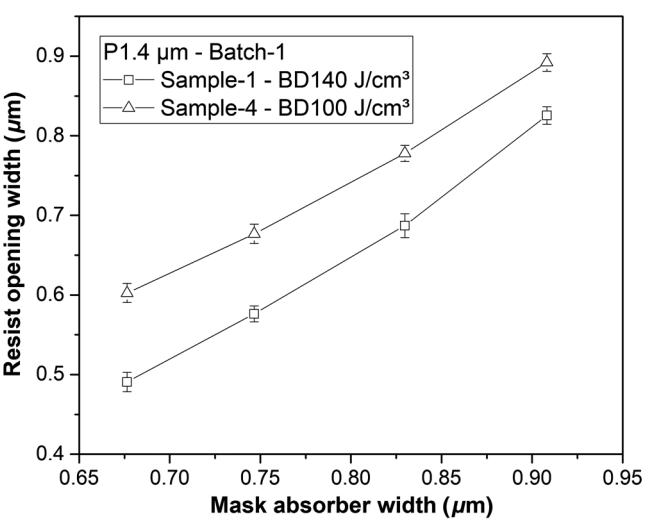

Fig. 14 Graphical comparison of resist opening widths achieved from corresponding absorber widths on the mask for period 1.4 μm with two bottom-doses 100 and 140 J/cm^3 between sample-1 and sample-4.

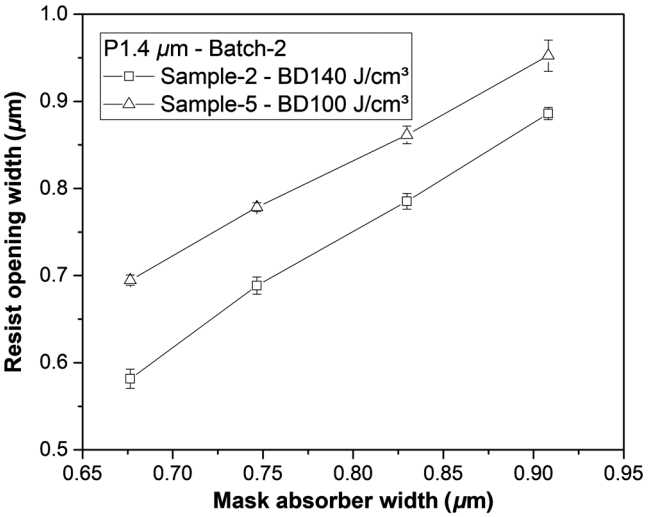

Fig. 15 Graphical comparison of resist opening widths achieved from corresponding absorber widths on the mask for period 1.4 μm with two bottom-doses 100 and 140 J/cm^3 between sample-2 and sample-5.

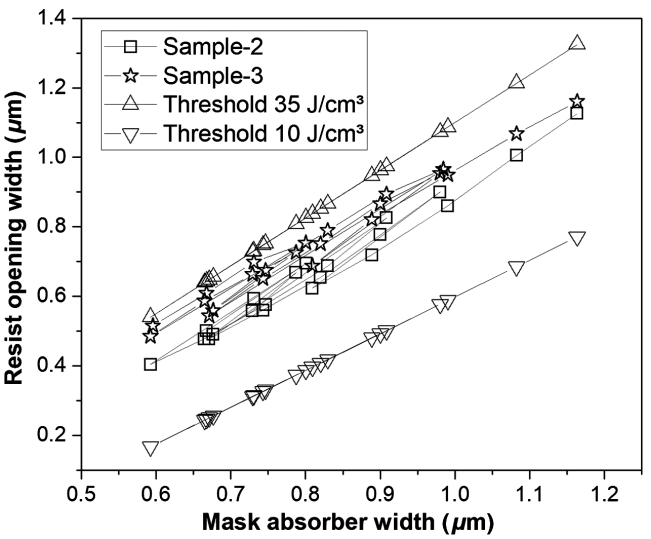

Fig. 16 Comparative analysis between the simulation and experimental results for the sample-2 and sample-3.

smaller mask absorber width; the value is ~6% (50 nm) for larger absorber width. Using a lower bottom-dose seems to be more appropriate to obtain the desirable structure dimensions similar to the mask. Using a smaller bottom-dose also minimizes the possibilities of having residual resist at the bottom of the structures in the unexposed regions. In contrast, for thicker resist layers (larger than the 10 μm used here), the smaller bottom-dose could introduce instability.

6 Comparison: Experiment and Simulation

A comparative analysis between the experimental and simulation results was performed. In Fig. 16, an exemplary comparison is presented for the sample-2 and sample-3, and the corresponding simulated results.

The linear behavior is validated; furthermore, for the chosen threshold of 35 J/cm^3, the structural widths show good agreement with the simulated one. The agreement is better for the lower gold absorber width; this could be explained by the PEB process, which is not considered in the simulation but could introduce shrinkage in the resist structures. Another explanation is related to the gold absorber thickness, which could be less than 1 μm in some period fields; in this case, the dose deposited underneath the gold absorber will not be negligible anymore and will lower the structural opening.

A lower bottom-dose of 100 J/cm^3 produced 6% to 16% larger resist openings (smaller deviation from mask to sample) compared to 140 J/cm^3 for 1.4-μm period microstructure fields; this is also validated by the simulation; even if the calculated deviation is lower. Nevertheless, the value belong to the interval of the measurement/simulated uncertainty ($\pm$50 nm due to the 100 nm $\times$ 100 nm grids for the simulation, $\pm$40 nm due to the analysis SEM pixel size in the images).

7 Conclusion

In this paper, simulated and experimental results were presented to demonstrate the possibilities of fabricating sub-μm structures, considering the secondary effects during x-ray exposure. Samples with a low thickness of 10 μm were tested experimentally. For two separate batches of resist, the final structural widths showed a constant deviation from mask to sample, independent of the period; this validates our simulation. When the samples from the two batches of resist were compared to each other, a considerable change in contrast of >10% was observed for the same mr-X 10 resist formulation; this is validated in the simulation by taking into account different dose threshold. We demonstrate that the simulation program could be used to design a period with its DC, within the mentioned uncertainty. Experimentally, we can fabricate microstructures with 1.2 μm minimum period (resist width of ~700 nm) and height of ~10 μm using the ANKA/KARA LIGA-1 beamline. The stability of the lamellae on one hand could be enhanced by decreasing their length and increasing the number of bridges, and on the other hand by using a low absorbing layer/substrate with high roughness such as graphite wafer. Further experiments will be performed in this direction, and the electroplating step will be added accordingly.

Acknowledgments

This work was supported by JST ERATO (Grant No. JPMJER1403) and by BMBF via ZIM under Contract No. KF2780302. The authors are thankful for the support of the Karlsruhe Nano Micro Facility (KNMF), a Helmholtz Research Infrastructure at Karlsruhe Institute of Technology (KIT), and the Karlsruhe School of Optics and Photonics (KSOP).

References

1. W. Menz, J. Mohr, and O. Paul, *Microsystem Technology*, pp. 289–380, Wiley-VCH Verlag GmbH, Weinheim (2001).
2. V. Saile, "Introduction: LIGA and its applications," in *LIGA and Its Applications*, V. Saile et al., Eds., Vol. **7**, pp. 1–10, Wiley-VCH Verlag GmbH, Weinheim (2009).
3. P. Meyer and J. Schulz, "Deep x-ray lithography," Chapter 16 in *Micromanufacturing Engineering and Technology*, Y. Qin, Ed., pp. 365–391, 2nd ed., Elsevier Inc., Boston, Massachusetts (2015).
4. J. Goettert et al., "Soft x-ray lithography for high-aspect ratio submicrometer structures," in *Nanotech Conf. and Expo*, Vol. 2, pp. 188–191 (2012).

5. T. Mappes, S. Achenbach, and J. Mohr, "Process conditions in x-ray lithography for the fabrication of devices with sub-micron feature sizes," *Microsyst. Technol.* **13**(3–4), 355–360 (2007).
6. A. Momose, "Phase-sensitive imaging and phase tomography using x-ray interferometers," *Opt. Express* **11**(19), 2303–2314 (2003).
7. T. Weitkamp et al., "X-ray phase imaging with a grating interferometer," *Opt. Express* **13**, 6296–6304 (2005).
8. F. Pfeiffer et al., "Grating-based x-ray phase contrast for biomedical imaging applications," *Z. Med. Phys.* **23**(3), 176–185 (2013).
9. E. Reznikova et al., "Soft x-ray lithography of high aspect ratio SU8 submicron structures," *Microsyst. Technol.* **14**(9), 1683–1688 (2008).
10. P. Meyer, "Fast and accurate x-ray lithography simulation enabled by using Monte Carlo method. New version of DoseSim: a software dedicated to deep x-ray lithography (LIGA)," *Microsyst. Technol.* **18**, 1971–1980 (2012).
11. J. Kouba et al., "SU-8: promising resist for advanced direct LIGA applications for high aspect ratio mechanical microparts," *Microsyst. Technol.* **13**(3–4), 311–317 (2006).
12. P. Meyer, J. Schulz, and L. Hahn, "DoseSim: Microsoft-Windows graphical user interface for using synchrotron x-ray exposure and subsequent development in the LIGA process," *Rev. Sci. Instrum.* **74**(2), 1113–1119 (2003).
13. G. Aigeldinger, "Implementation of an ultra deep x-ray lithography system at CAMD," PhD Thesis, University Freiburg (2001).
14. D. Kunka et al., "Characterization method for new resist formulations for HAR patterns made by x-ray lithography," *Microsyst. Technol.* **20**(10–11), 2023–2029 (2014).
15. F. Koch et al., "Increasing the aperture of x-ray mosaic lenses by freeze drying," *J. Micromech. Microeng.* **25**(7), 075015 (2015).

Abrar Faisal is a PhD candidate at the Institute of Microstructure Technology at KIT, Germany. He received his BSc degree in electrical and electronic engineering and MEng degree in telecommunications from American International University-Bangladesh in 2009 and 2011, respectively. After working as a lecturer for two years, he pursued his MSc degree in optics and photonics at Karlsruhe Institute of Technology in 2015. His research interests include micro- and nanofabrication based on evolving lithographic technologies.

Thomas Beckenbach earned an engineering degree in 2009; he studied sensor applications. Since 2010, he has worked for the company microworks GmbH, which focuses on the production of high-precision parts using x-ray-LIGA technology. He leads the engineering group.

Jürgen Mohr has led the x-ray lithography and microoptics IMT/KIT department since 1992 and since 2010 he has served as spokesperson for the Helmholtz Research Infrastructure KNMF. He has pioneered work on deep x-ray lithography, and is a world-wide recognized expert in micro-fabrication and microoptics. He is coauthor of one textbook and has more than 200 publications in international journals. Today his research focuses on the fabrication of x-ray optical components for imaging applications.

Pascal Meyer obtained his PhD from the University of Franche-Comté in 1996. After two years as an assistant professor at the Franche-Comté University, he started as a postdoc at the IMT/KIT in 1998, where he is now leading the gratings fabrication group using deep-x-ray lithography.